International Journal of Pharmaceutics 376 (2009) 134–140

Contents lists available at ScienceDirect

International Journal of Pharmaceutics

journal homepage: www.elsevier.com/locate/ijpharm

Pharmaceutical Nanotechnology

# pH-sensitive properties of surface charge-switched multifunctional polymeric micelle

Kyung Taek Oh[a], Dongin Kim[b], Hyeon Hee You[c], Yong Sik Ahn[c], Eun Seong Lee[c,*]

[a] College of Pharmacy, Chung-Ang University, 221 Heukseok dong, Dongjak-gu, Seoul 155-756, Republic of Korea
[b] The Wallace H. Coulter Department of Biomedical Engineering and Parker H. Petit Institute for Bioengineering and Bioscience, Georgia Institute of Technology, Atlanta, GA 30332, USA
[c] Division of Biotechnology, The Catholic University of Korea, 43-1 Yeokgok 2-dong, Wonmi-gu, Bucheon-si, Gyeonggi-do 420-743, Republic of Korea

ARTICLE INFO

*Article history:*
Received 4 March 2009
Received in revised form 14 April 2009
Accepted 16 April 2009
Available online 24 April 2009

*Keywords:*
pH-responsive polymeric micelle
pH-triggered surface charge switching
2,3-Dimethyl maleic aicd
Poly(L-histidine)

ABSTRACT

A surface charge-switched polymeric micelle with a pH signal was developed as a drug-carrying nanovehicle for tumor targeting. The micelles (particle size: ~85 nm), constructed from poly(L-lactic acid)-*b*-poly(ethylene glycol)-*b*-poly(L-lysine-$N^{\varepsilon}$-(2,3-dimethyl maleic acid)) (PLA-*b*-PEG-*b*-PLys-DMA) and formed by self-assembly in an aqueous pH 7.4 solution, consisted of a hydrophobic core (PLA core) and two hydrophilic shells (PEG shell and PLys-DMA shell). An anionic charge can be built on the surface of the micelle at a physiological pH (~pH 7.4) due to 2,3-dimethyl maleic acid (DMA). However, DMA becomes chemically dissociated from the micelle under mild acidic conditions (pH 6.5–7.0) such as that found in solid tumors, which results in the formation of a cationic surface due to the poly(L-lysine) (PLys). This pH-triggered switch in surface charge may enhance cellular uptake of micelles to solid tumors, via an adsorptive endocytotic pathway due to the electrostatic interaction between micelles and cells. In addition, blending of the poly(L-histidine) (polyHis) into the hydrophobic core provides a mechanism for endosomal pH-triggered drug-release from the polymeric micelle. These combined properties of the polymeric micelle may aid in tumor-specific drug accumulation and allow it to be used as an effective treatment for tumors.

© 2009 Elsevier B.V. All rights reserved.

## 1. Introduction

Chemotherapy still remains the primary modality for treating tumors. One of the most important factors dictating the success of chemotherapy is controlling the dose such that the beneficial anticancer activity is balanced with the negative toxicity effects (Campbell, 2006; Ferrari, 2005; Ferrari et al., 2005; Rothenberg et al., 2003; Maeda et al., 2000). Currently, one of the most significant problems with chemotherapy is damage to surrounding healthy organs and tissue because many anticancer drugs are simply designed to destroy cells. The threat of severe side effects caused by the random distribution of the drugs has prevented the use of maximum dosages, which has ultimately decreased the therapeutic activity of the drug (Campbell, 2006; Ferrari, 2005; Ferrari et al., 2005; Rothenberg et al., 2003). In this respect, it is important to minimize cytotoxic effect on normal tissues while maximizing drug accumulation at the site of action (tumors), which is undeniably relevant for the development of tumor-specific targeting systems (Oh et al., 2007; Duncan, 2006).

Solid tumors are often characterized by specific receptors or antigens on cell surfaces (Duncan, 2006; Parker et al., 2005; Daniels et al., 2005). Receptors or antigens provide uptake routes for nutrients and signals from the surrounding environment, which are essential for active growth of tumor cells (Parker et al., 2005). Drug carriers exploit these uptake pathways by presenting tumor-specific ligands or antibodies on the surface, which is purposed to improve the efficacy of the anticancer drug for the elimination of tumors (Alexis et al., 2008; Lavasanifar et al., 2002). However, this application is not often effective in the clinical phase because tumors usually display heterogeneous cell populations as wells as differential receptor or antigen expression on cell surfaces (Duncan, 2006; Parker et al., 2005; Daniels et al., 2005).

Unlike the complex issues associated with targeting the phenotype of tumor cells, pH differences between the solid tumor area and normal tissue (or blood) is relatively simple and intrinsic (Gillies et al., 2004; Gillies and Frechet, 2005; Hobbs et al., 1998; Stubbs et al., 2000; Tannock and Rotin, 1989). The extracellular pH of normal tissue ($pH_e$) or blood pH is typically 7.4. The average pH for readily accessible tumor areas like the limbs, neck, chest, and head for various solid tumors (such as adenocarcinoma, squamous cell carcinoma, soft tissue sarcoma, and malignant melanoma) has been reported to be 7.06 (van Sluis et al., 1999; Leeper et al., 1994; Gillies et al., 2004). In addition, 80% of all measured tumor $pH_e$

* Corresponding author. Tel.: +82 2 2164 4921; fax: +82 2 2164 4865.
*E-mail address:* hejulu@hanmail.net (E.S. Lee).

0378-5173/$ – see front matter © 2009 Elsevier B.V. All rights reserved.
doi:10.1016/j.ijpharm.2009.04.021

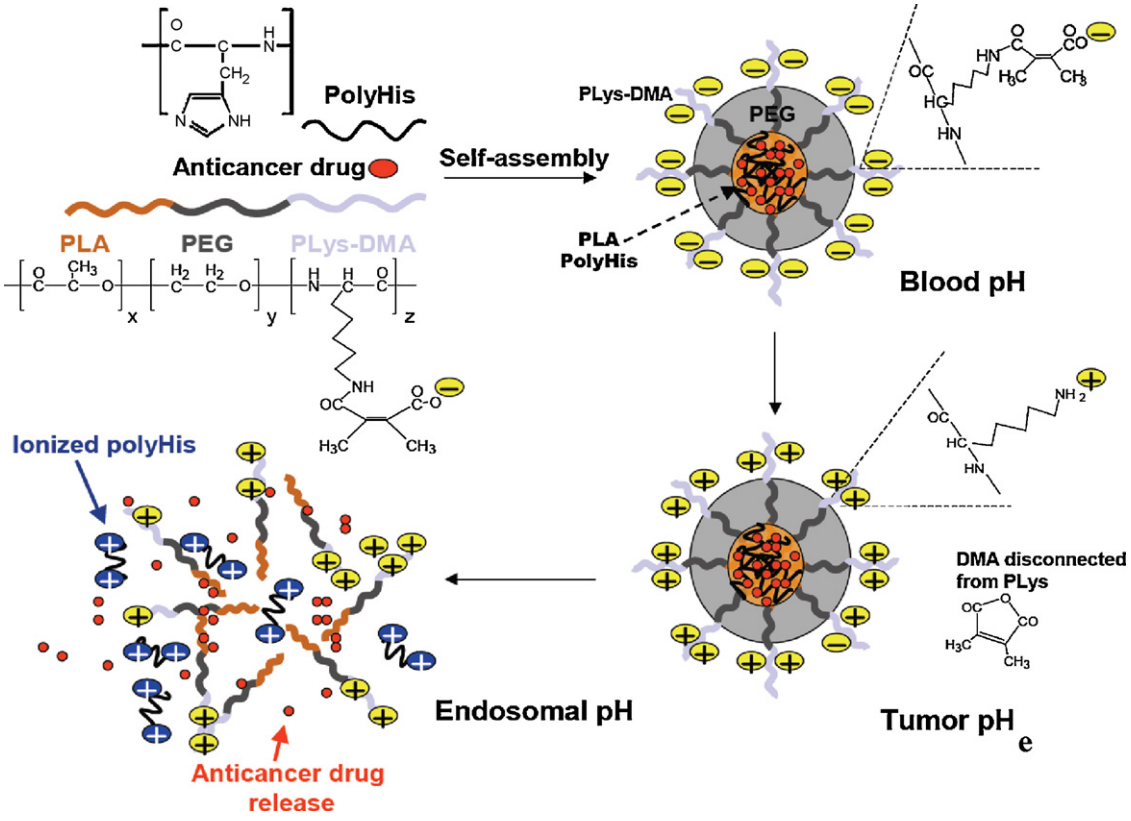


**Fig. 1.** Schematic diagram depicting the central concept.

values range from pH 7.0 and 6.5 (Ojugo et al., 1999; van Sluis et al., 1999). Moreover, the tumor $pH_e$ can be lowered by 0.2–0.4 pH units when glucose is given orally or intravenously in patients (Leeper et al., 1994; Volk et al., 1993). Smart drug carriers that respond to pH stimuli can thus be potentially used for tumor-specific anticancer drug delivery (Lee et al., 2003, 2005a,b, 2007a, 2008a,b; Lee and Youn, 2008; Kim et al., 2005, 2008; Kataoka et al., 2001; Bae et al., 2005; Na et al., 2007; Oh and Lee, 2008; Sawant et al., 2006).

Recently, we reported on the development of super pH-responsive multifunctional micelles containing non-specific ligands (such as biotin and Tat peptide) that can be repositioned on the surface of the micelle (Lee et al., 2005b, 2008b). Non-specific ligands anchored to the hydrophobic core were masked by the PEG shell at physiological pH (~pH 7.4), but non-specific ligands moved to the surface of the PEG shell when the pH was decreased below 7.0, which mediated endocytosis of the micelles by solid tumors under mild acidic conditions (pH 6.5–7.0). When the pH was lowered further (pH < 6.5), the micelle disintegrated and released drugs contained in the core. This multi-functionality has been expected to replace the need for cell-specific antibodies or targeting ligands, thereby providing a general strategy for solid tumor targeting (Lee et al., 2005a,b, 2008a,b).

In this study, we newly designed a pH-triggered surface charge-switched polymeric micelles from amphiphilic biodegradable PLA-*b*-PEG-*b*-PLys-DMA block copolymers. As shown in Fig. 1, the polymeric micelles contain an anionic surface due to the presence of DMA on the PLys shell at pH 7.4; however, the DMA will chemically dissociate at tumor $pH_e$, resulting in the formation of polycationic micelles. This micelle then may be effectively internalized by tumor cells via an adsorptive endocytosis that does not need any ligands (Huang et al., 2002). This process will be initiated by a nonspecific physical adsorption of micelles to the cell surface by electrostatic force. Moreover, polyHis was blended with the PLA block in the hydrophobic core, which was expected to lead to pH-triggered drug-release from the polymeric micelle due to ionization at endosomal pH (Lee et al., 2005a,b, 2007a, 2008a,b). To experimentally demonstrate this concept, we examined the pH-sensitive properties of this system and monitored the release behavior of pH-dependent anticancer drugs at low pH.

## 2. Materials and methods

### 2.1. Materials

$N^{\varepsilon}$-Benzyloxycarbonyl-L-lysine, 2,3-dimethyl maleic anhydride (DMA), *N*-(2-aminoethyl) maleimide (AEM), triphosgene, triethylamine (TEA), anhydrous dioxane, trifluoroacetic acid (TFA), tetramethylsilane (TMS), diethyl ether, dimethylformamide (DMF), 33% HBr in acetic acid, doxorubicin·HCl (DOX·HCl), pyrene, HCl, NaOH, $Na_2B_4O_7$, and dimethylsulfoxide (DMSO) were purchased from Sigma–Aldrich (St. Louis, MO, USA). Thiolated PLA ($M_n$ 3K)-*b*-PEG (Mn 2K) (PLA3K-*b*-PEG2K-SH) and polyHis (Mn 5K) (polyHis5K) were synthesized as described in detail in our previous reports (Lee et al., 2003, 2007a, 2008b; Oh and Lee, 2008). Briefly, PLA3K-*b*-PEG2K-COOH was prepared by ring-opening polymerization of L-lactide at 110 °C using mono-carboxyl terminated PEG2K (PEG2K-COOH) (Lee et al., 2003) as an initiator. Next, PLA3K-*b*-PEG2K-COOH pre-activated with *N*-hydroxysuccinimide (Sigma–Aldrich) and *N*,*N*′-dicyclohexylcarbodiimide (Sigma–Aldrich) was reacted with cystamine (Sigma–Aldrich). Triscarboxyethylphosphine (Sigma–Aldrich) dissolved in deionized water was mixed with the solution for the reduction of PLA-*b*-PEG-cystamine-PEG-*b*-PLA or PLA-*b*-PEG-cystamine. This procedure yielded PLA3K-*b*-PEG2K-SH. PolyHis5K was synthesized by ring-opening polymerization of L-histidine *N*-carboxyanhydride (NCA)·HCl at room temperature using isopropylamine (Sigma–Aldrich) as an initiator.

### 2.2. Polymer synthesis

Poly($N^{\varepsilon}$-benzyloxycarbonyl-L-lysine) was synthesized by ring-opening polymerization of *N*-carboxy-($N^{\varepsilon}$-benzyloxycarbonyl)-L-lysine anhydride (L-lysine NCA) using AEM as a initiator as described by van Dijk-Wolthuis et al. (1997). Briefly, L-lysine NCA (40 mmol) prepared in anhydrous dioxane at 65 °C was dissolved in anhydrous DMF (20 ml) in the presence of AEM (1 or 2 mmol: corresponding with a molar NCA: initiator ratio of 40 or 20) and polymerized for 3 days at room temperature. After the reaction was completed, poly($N^{\varepsilon}$-benzyloxycarbonyl-L-lysine) was obtained following re-precipitation from excess diethyl ether. To remove the benzyloxylcarbonyl group from the polymer, poly($N^{\varepsilon}$-benzyloxycarbonyl-L-lysine) (1.5 g) was dissolved in TFA (5 ml) and then mixed with 33% HBr in acetic acid (5 ml) at room temperature for 30 min. Poly(L-lysine) (PLys)·HBr was recrystallized from excess diethyl ether/ethanol (50/50 vol.%). Removal of the benzyloxylcarbonyl group was confirmed by $^1$H NMR (DMSO-$d_6$ with TMS) peaks: no peak of $\delta$ 7.40–7.21 (benzyl group) (data not shown). The molecular weight of PLys was estimated from $^1$H NMR (DMSO-$d_6$ with TMS) peaks using the integration ratio of the peaks from the repeating unit (–CH–, $\delta$ 4.72) and the initiator (–CH=CH–, $\delta$ 6.92) (data not shown). The molecular weight of PLys was 2054 (2K) and 4929 (5K) Daltons. Subsequently, PLys ($M_n$ 2K or 5K) (PLys2K or PLys5K) (0.5 mmol) was reacted with DMA (30 mmol) in DMSO (20 ml) at room temperature for 2 days. After the reaction was completed, the solution was transferred to a pre-swollen dialysis membrane tube (Spectra/Por; MWCO 2K) and was dialyzed against deionized water to remove unconjugated DMA for 3 days. The resulting solution was freeze-dried for 2 days. The DMA conjugation was confirmed by the presence of $^1$H NMR (DMSO-$d_6$ with TMS) peak at $\delta$ 1.95 (–$CH_3$, DMA) (data not shown). The percent conjugation was 95 ± 4% and the molecular weight of PLys-DMA was 3962 and 9887 Daltons, as calculated by the comparison of two $^1$H NMR peaks ($CDCl_3$ with TMS) [$\delta$ 4.76 (–CH–, repeating unit) and $\delta$ 1.95 (–$CH_3$, DMA)] (data not shown). The coupling of PLys-DMA and PLA3K-*b*-PEG2K-SH was carried out in DMF overnight. Excess diethyl ether was then added to precipitate PLA3K-*b*-PEG2K-*b*-PLys-DMA. The complete coupling of PLys-DMA and PLA3K-*b*-PEG2K-SH was confirmed (Fig. 2) by the change of $\delta$ 6.94 (–CH=CH–, $^1$H NMR) to $\delta$ 3.34 (–CH–$CH_2$–) at the terminal maleimide of PLys (data not shown).

### 2.3. Micelle preparation

Each block copolymer (100 mg) or blended block copolymers with different weight ratios (100/0, 70/30, 50/50, and 25/75 wt.% of PLA-*b*-PEG-*b*-PLys-DMA to polyHis5K) dissolved in DMSO (20 ml) was transferred to a pre-swollen dialysis membrane tube (Spectra/Por; MWCO 15K) and dialyzed against HCl (or NaOH)–$Na_2B_4O_7$ buffer solution (pH 8.0, 0.5 mM) for 24 h (Lee et al., 2003, 2007a, 2008b; Oh and Lee, 2008). The outer phase was replaced three times with fresh $Na_2B_4O_7$ buffer solution. The solution was subsequently lyophilized after filtering through a 0.8 μm syringe filter. The yield (wt.%) of micelles was 83 ± 7 wt.%, as calculated by weighing the freeze-dried micelle powder.

### 2.4. Photon correlation spectroscopy (PCS) by Zetasizer

PCS was conducted using a Zetasizer 3000 (Malvern Instruments, USA) equipped with a He–Ne Laser beam at a wavelength of 633 nm and a fixed scattering angle of 90°. The polymeric micelles (0.1 g/l, ionic strength: 0.15) were exposed to different pH conditions (pH 7.4–5.5) at 37 °C for 24 h before measuring the particle size and particle size distribution.

### 2.5. Critical micelle concentration (CMC) determination

A freeze-dried micelle sample was dispersed in HCl (or NaOH)–$Na_2B_4O_7$ buffer solution (pH 7.4, ionic strength: 0.15). The micellar solution ($1 \times 10^{-4}$–$1 \times 10^{-1}$ g/l) was mixed with pyrene (fluorescence probe) at 50 °C for 6 h, yielding a final pyrene concentration of $6.0 \times 10^{-7}$ M. The fluorescence measurement was performed using a Shimadzu RF-5301PC Spectrofluorometer. The pyrene emission at $\lambda_{ex}$ 339 nm was recorded. The CMC was estimated by plotting $I_1$ (intensity of first peak) of the emission spectra profile against of the log of the micelle concentration. The CMC of each micelle was determined from the crossover point at low polymer concentration in this plot (Lee et al., 2003, 2007a; Oh and Lee, 2008).

### 2.6. Zeta potential

Zeta potential was measured using a Zetasizer 3000 (Malvern Instruments, USA). The zeta potential of each micelle (0.5 g/l) at

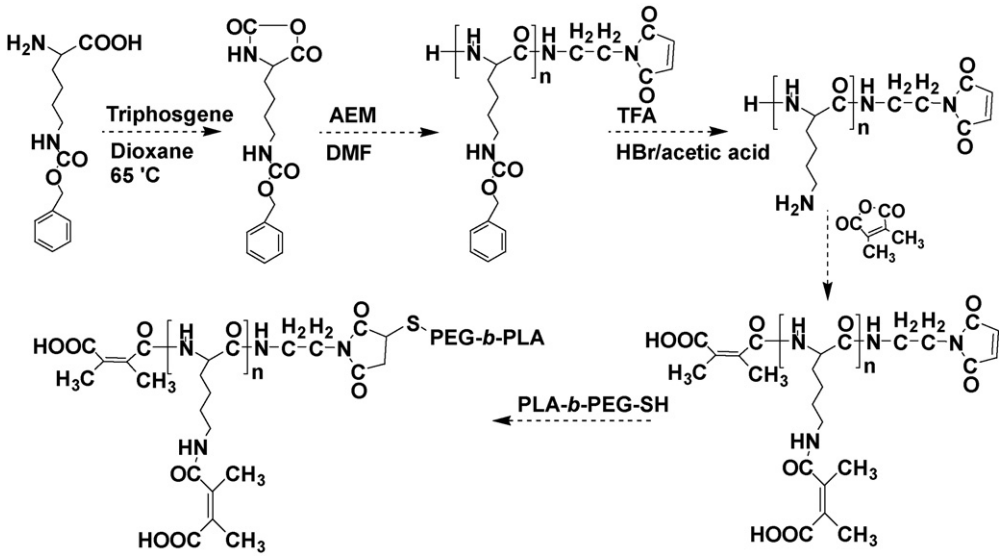


**Fig. 2.** Overall synthesis scheme of PLA-*b*-PEG-*b*-PLys-DMA.

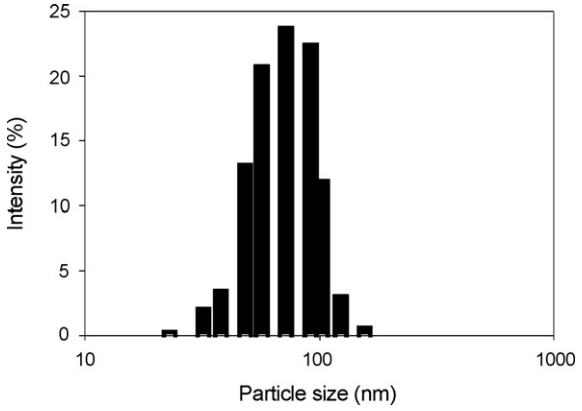


**Fig. 3.** Particle size distribution of PLA3K-*b*-PEG2K-*b*-PLys2K-DMA micelles in PBS solution (ionic strength: 0.15, pH 7.4).

different pHs (pH 7.4–6.0, 10 mM PBS) was recorded as a function of time (0–250 min).

### 2.7. Transmittance of micellar solution

The transmittance was measured using a Varian CARY 1E UV–vis spectrophotometer. Before the test, all micellar solutions (0.1 g/l, ionic strength: 0.15) with different pHs (pH 7.4–5.5) were stabilized at 37 °C for 24 h. Relative transmittance of the micellar solution was measured in the selected pH change with respect to the transmittance at pH 7.4.

### 2.8. DOX loading

When a total of 5 mg of polymer with DOX (1 mg) was dialyzed to produce micelles, 0.82–0.92 mg of DOX was encapsulated within the micelles. The amount of entrapped DOX was determined by measuring the UV absorbance at 481 nm of the drug-loaded polymeric micelles dissolved in DMSO as described previously (Lee et al., 2003, 2007a, 2008b; Oh and Lee, 2008).

### 2.9. DOX release

DOX-loaded micelles were dispersed in PBS (1 ml, ionic strength: 0.15) at different pHs (pH 7.4–5.5), and then transferred to a dialysis membrane tube (Spectra/Por MWCO 5K). The membrane tube was immersed in a vial containing 10 ml of phosphate buffered saline (PBS) solution adjusted to different pHs (pH 7.4–5.5). The release of DOX from the micelles was measured with mechanical shaking (100 rev./min) at 37 °C. The outer phase of the dialysis membrane was withdrawn and replaced with fresh buffer solution at predetermined time intervals in order to maintain the sink condition. The measurement of DOX concentration by an UV/vis spectrophotometer was performed after adjusting each solution pH to 8.0 using a 0.1 M NaOH solution (Lee et al., 2003, 2007a, 2008b; Oh and Lee, 2008).

## 3. Results and discussion

### 3.1. Preparation of polymeric micelles

A new polyelectrolyte block copolymer (PLA-*b*-PEG-*b*-PLys-DMA) consisting of a hydrophobic block (PLA), hydrophilic inner block (PEG), and hydrophilic outer block (electronic PLys-DMA) was successfully produced (Fig. 1). The PLys-DMA block was prepared by grafting DMA to the pendant amine group in PLys (Fig. 2). The purpose of masking PLys with DMA was to develop an anionic poly(amino acid). Coupling a thiol group (–SH) at the end of PLA-*b*-PEG to the maleimide of PLys-DMA was the last step in the preparation of PLA-*b*-PEG-*b*-PLys-DMA.

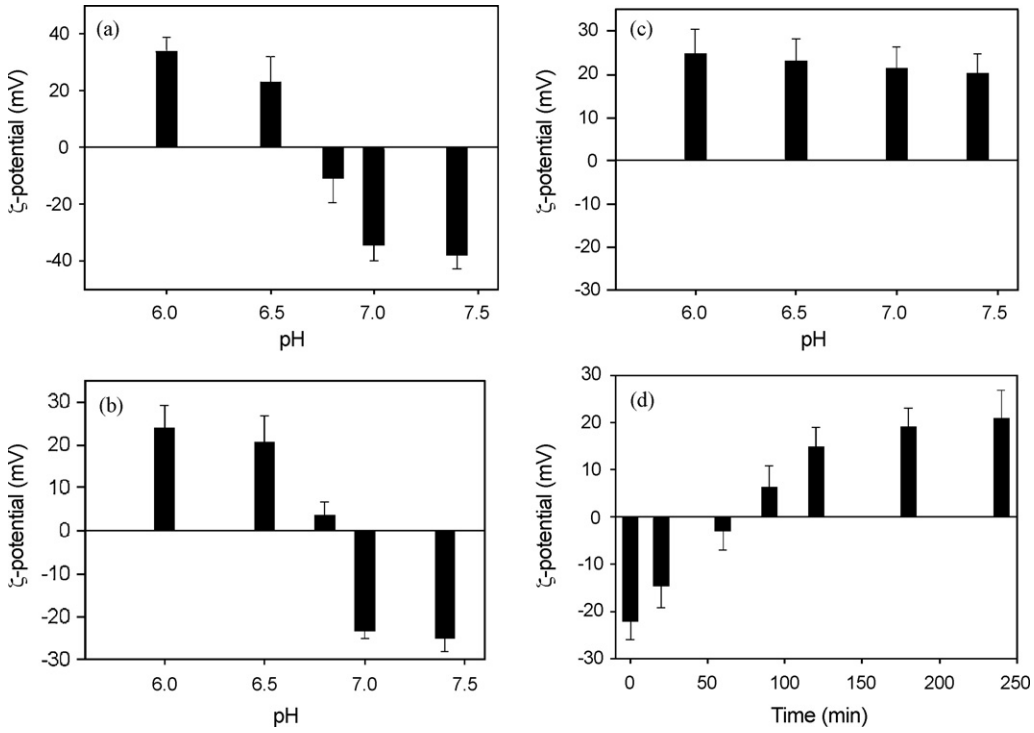


**Fig. 4.** Zeta-potential charges ($n = 3$) of (a) PLA3K-*b*-PEG2K-*b*-PLys5K-DMA micelles, (b) PLA3K-*b*-PEG2K-*b*-PLys2K-DMA micelles, and (c) PLA3K-*b*-PEG2K-*b*-PLys2K micelles at different pHs. The pH of each micellar solution (0.5 mg/ml, 10 mM PBS) was maintined for 4 h. (d) Time-dependent surface charges ($n = 3$) of PLA3K-*b*-PEG2K-*b*-PLys2K-DMA micelles (0.5 mg/ml, 10 mM PBS) at pH 6.5 solution. All micelles were stabilized at each pH for 10 min prior to measuring the zeta-potential.

To investigate the colloidal properties of the polymeric micelles, the micelles were preformulated with PLA-*b*-PEG-*b*-PLys-DMA using the diafilteration method (Lee et al., 2003). The average size of the PLA3K-*b*-PEG2K-*b*-PLys2K-DMA micelles was about 85 nm and these particles displayed a unimodal size distribution (Fig. 3). Similar results were observed for the PLA3K-*b*-PEG2K-*b*-PLys5K-DMA micelles, which had an average size of 92 nm and also displayed a unimodal size distribution (data not shown). In addition, blending PLA3K-*b*-PEG2K-*b*-PLys2K (or 5K)-DMA with polyHis5K at different mixing ratios (100/0, 70/30, 50/50, 25/75 wt.%) did not significantly affect the average micelle size (data not shown). Furthermore, there was no evidence of micelle aggregation (no change in particle size) for the micelles prepared in this study over a period of 7 days.

### 3.2. pH-triggered surface charge switching

The pH-sensitive feature of the micellar surface was assessed by the zeta-potential analysis (Fig. 4). As the pH of the micellar solution decreased from pH 7.4 to 6.5, the zeta-potential of the PLA3K-*b*-PEG2K-*b*-PLys5K-DMA micelles (Fig. 4(a)) increased from −37 to 22 mV, indicating removal of the anionic DMA from the cationic PLys. The zeta-potential of the PLA3K-*b*-PEG2K-*b*-PLys2K-DMA micelles also displayed a similar trend, where it increased from −25 (pH 7.4) to 20 mV (pH 6.5) depending on the molecular weight of PLys-DMA block (Fig. 4(b)). The zeta-potential for the PLA3K-*b*-PEG2K-*b*-PLys2K micelle remained the same at all pHs tested (Fig. 4(c)). These results were comparable with that obtained when citraconic acid (CA) was grafted to aminated pendant group of poly(L-aspartic acid) at pH 7.4, which was chemically dissociated from poly(L-aspartic acid) at pH 5.5 not at tumor $pH_e$ (pH 7.0–6.5); this system (engineered for the complexation with lysozyme) only switched the surface charge of poly(L-aspartic acid) from anionic above pH 5.5 to cationic at pH 5.5 (Lee et al., 2007b). Furthermore, the zeta-potential of the micelles at pH 6.5 displayed a sharply transition from −22 to 15 mV in 120 min, which plateaued after 180 min (Fig. 4(d)). This DMA dissociation kinetics data suggest that the micelle should remain in a mild acidic condition like tumor $pH_e$ for at least for 2–3 h, in order to enhance micellar uptake in tumor cells. Overall, these results demonstrate that the PLA3K-*b*-PEG2K-*b*-PLys-DMA micelle was capable of distinguishing tumor extracellular $pH_e$ by a pH-triggered switch in surface charge and the shielding/deshielding process of the PLys block.

### 3.3. pH-triggered drug release

PolyHis was blended with PLA3K-*b*-PEG2K-*b*-PLys2K-DMA at different weight ratios during the preparation of the polymeric micelles. Herein, polyHis was used as an actuator for controlling the disintegration of the hydrophobic core at endosomal pH (< pH 6.5) (Lee et al., 2005a,b, 2007a) (Fig. 1). This is consistent with the report that the PEG-*b*-polyHis-*b*-PLA-*b*-PEG tetra-block micelles, constituted for endosomal pH targeting, were destabilized at pH 6.4 due to the concurrent ionization of the polyHis (Oh and Lee, 2008). In this study, the PLA3K-*b*-PEG2K-*b*-PLys2K-DMA micelle without polyHis5K was stable at all pHs tested; no change in particle size was observed over 24 h (Fig. 5(a)). However, as the polyHis5K content in the micelles increased, the average micelle size gradually increased, especially at pH 6.0. This observation seems to be associated with the ionization of polyHis5K ($pK_b \sim 6.4$), accompanied by separation and isolation of PLA3K-*b*-PEG2K-*b*-PLys2K from the micelles, which in turn became segregated in water due to the hydrophobic PLA block (Lee et al., 2003, 2005a,b). In particular, 50/50 wt.% blending of polyHis5K and PLA3K-*b*-PEG2K-*b*-PLys2K-DMA considerably enhanced the destabilization of the micelle (or demicellization) at pH 6.0, while preserving the micelle stability at pH 7.4–6.5 (Fig. 5(a)). This results is consistent with the notion that

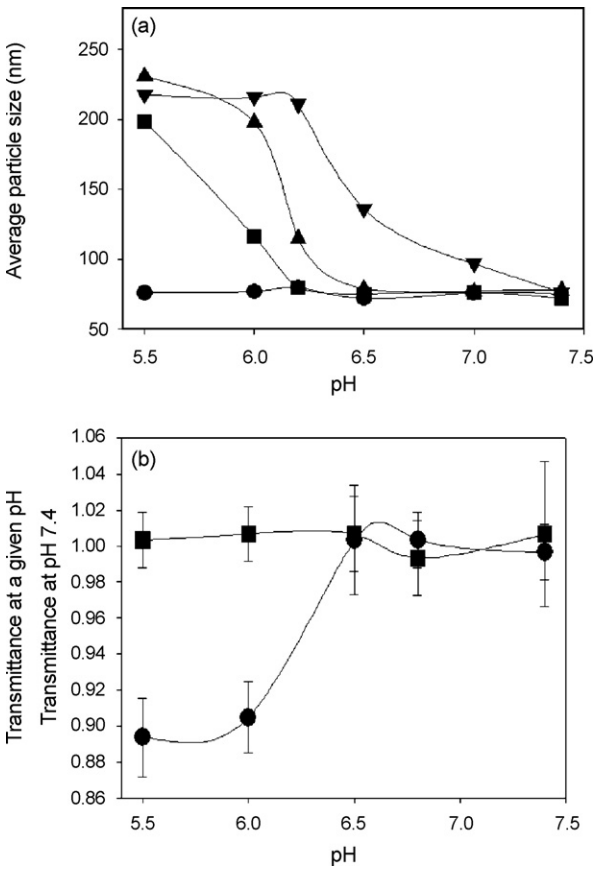


**Fig. 5.** (a) Change in particle size of PLA3K-*b*-PEG2K-*b*-PLys2K-DMA/polyHis5K mixed micelle at different pHs ($n = 3$) after 24 h. Weight ratios of PLA3K-*b*-PEG2K-*b*-PLys2K-DMA/polyHis5K were 100/0 wt.% (●), 70/30 wt.% (■), 50/50 wt.% (▲), and 25/75 wt.% (▼). (b) Change in relative transmittance of PLA3K-*b*-PEG2K-*b*-PLys2K-DMA/polyHis5K mixed micelle (50/50 wt.%) (●) and PLA3K-*b*-PEG2K-*b*-PLys2K-DMA micelle (■) at different pHs ($n = 3$) after 24 h.

these mixed micelles have a decreased turbidity at pH 6.0 compared to that at pH 7.4–6.5 (Fig. 5(b)).

Fig. 6 shows the CMC value of each micelle at physiological pH (~pH 7.4). A fluorometry method using pyrene as the fluorescent probe was used to evaluate the CMC of each micelle (Lee

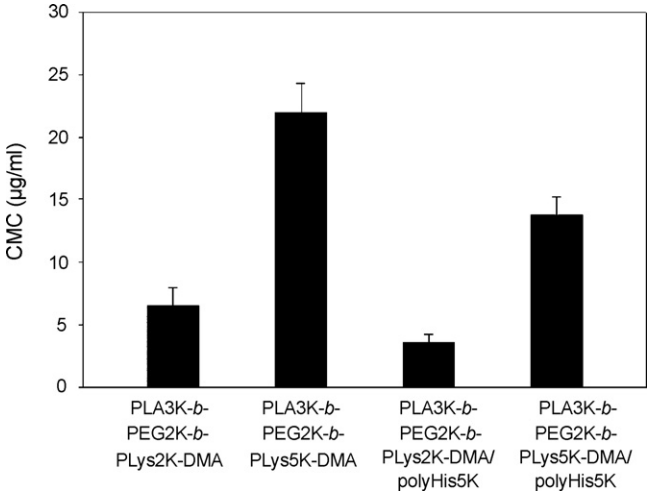


**Fig. 6.** CMC of each micelle [PLA3K-*b*-PEG2K-*b*-PLys2K-DMA micelle, PLA3K-*b*-PEG2K-*b*-PLys5K-DMA micelle, PLA3K-*b*-PEG2K-*b*-PLys2K-DMA/polyHis5K mixed micelle (50/50 wt.%), PLA3K-*b*-PEG2K-*b*-PLys5K-DMA/polyHis5K mixed micelle (50/50 wt.%)] (ionic strength: 0.15, pH 7.4) ($n = 3$).

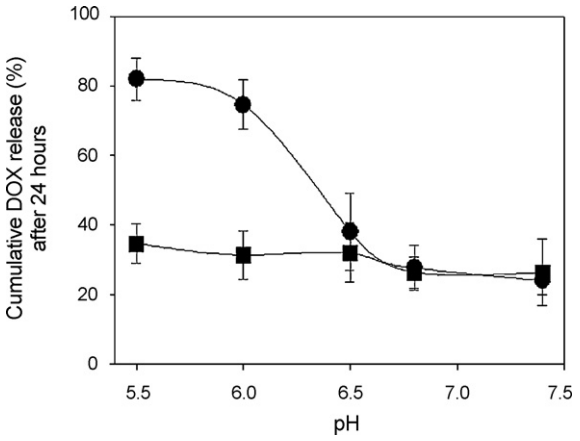


**Fig. 7.** DOX release from PLA3K-*b*-PEG2K-*b*-PLys2K-DMA/polyHis5K mixed micelle (50/50 wt.%) (●) and PLA3K-*b*-PEG2K-*b*-PLys2K-DMA micelle (■) at different pHs ($n = 3$) after 24 h.

et al., 2007a, 2008a,b; Oh and Lee, 2008). As the length of the hydrophilic block (PEG and PLys-DMA) increased, the CMC of the micelles increased due to the enhanced hydrophilicity. However, blending of polyHis5K decreased the CMC of mixed micelles by increasing the overall hydrophobicity in the hydrophilic-lipophilic balance (HLB). This result suggests that PLA3K-*b*-PEG2K-*b*-PLys2K-DMA/polyHis5K mixed micelles can be effectively used as a drug carrier by forming a stable structure (low CMC: ~3 μg/ml) in blood circulation (~pH 7.4) and by switching the surface charge of the carriers in response to tumor $pH_e$ (Fig. 4), which would result in enhanced drug accumulation in solid tumors. Furthermore, the mixed micelles localized in the endosomes after adsorptive endocytosis, may respond to endosomal pH (< pH 6.4), which may be accompanied by destabilization of the micelles (Fig. 5). As shown in Fig. 7, anticancer drug (DOX) release from the mixed micelles was accelerated at endosomal pH (~pH 6.0) due to the ionization of the polyHis5K and the destabilization of the hydrophobic core (Oh and Lee, 2008). In addition, the known proton buffering effect of polyHis (Lee et al., 2003, 2005a,b, 2007a, 2008a,b) is believed to be capable of physically disrupting endosomal membranes, which will aid in the transfer of the anticancer drugs from the endosome to the cytosol for effective apoptosis of tumor cells (Lee et al., 2003, 2005a,b; Rybak, 2008).

## 4. Conclusion

PLA-*b*-PEG-*b*-PLys-DMA and polyHis were blended for fabrication of a novel pH-triggered multifunctional polymeric micelle. The micelles, consisting of a hydrophobic core (PLA and polyHis) and hydrophilic shell (PEG and Plys-DMA), were designed to have a pH-triggered switch in surface charge from an anionic charge at a physiological pH (~pH 7.4) to a cationic charge at tumor $pH_e$. In addition, these novel polymeric micelles displayed a triggered release of anticancer drugs when the pH was decreased from pH 6.5 to 6.0 (endosomal pH). This polymeric micelle system, in principle, would have a very low level of micelle accumulation in normal tissue due to the charge repulsion effect that exists between the micelles with cells, while having a high probability of micelle accumulation in solid tumors due to the electrostatic interaction of micelles with cells. Thus, this would ultimately lead to endosomal pH-triggeried drug release after micelle internalization (adsorptive endocytosis). Of course, proof of this hypothesis will require further investigations including *in vitro*/*in vivo* efficacy evaluations and DMA toxicity tests.

## Acknowledgements

This work was supported by the Korea Research Foundation Grant funded by the Korean Government (KRF-2008-331-D00161) and by the Research Grant funded by the Gyeonggi Regional Research Center (GRRC).

## References

Alexis, F., Basto, P., Levy-Nissenbaum, E., Radovic-Moreno, A.F., Zhang, L., Pridgen, E., Wang, A.Z., Marein, S.L., Westerhof, K., Molnar, L.K., Farokhzad, O.C., 2008. HER-2-targeted nanoparticle-affibody bioconjugates for cancer therapy. Chem. Med. Chem. 3, 1839–1843.

Bae, Y., Nishiyama, N., Fukushima, S., Koyama, H., Yasuhiro, M., Kataoka, K., 2005. Preparation and biological characterization of polymeric micelle drug carriers with intracellular pH-triggered drug release property: tumor permeability, controlled subcellular drug distribution, and enhanced in vivo antitumor efficacy. Bioconjug. Chem. 16, 122–130.

Campbell, R.B., 2006. Tumor physiology and delivery of nanopharmaceuticals. Anti-Cancer Agents Med. Chem. 6, 503–512.

Daniels, R.A., Turley, H., Kimberley, F.C., Liu, X.S., Mongkolsapaya, J., Ch'En, P., Xu, X.N., Jin, B.Q., Pezzella, F., Screaton, G.R., 2005. Expression of TRAIL and TRAIL receptors in normal and malignant tissues. Cell Res. 15, 430–438.

Duncan, R., 2006. Polymer conjugates as anticancer nanomedicines. Nat. Rev. Cancer 6, 688–701.

Ferrari, M., 2005. Cancer nanotechnology: opportunities and challenges. Nat. Rev. Cancer 5, 161–171.

Ferrari, M., Barker, A., Downing, G., 2005. A cancer nanotechnology strategy. Nanobiotechnology 1, 129–131.

Gillies, E.R., Frechet, J.M., 2005. pH-responsive copolymer assemblies for controlled release of doxorubicin. Bioconjug. Chem. 16, 361–368.

Gillies, R.J., Raghunand, N., Garcia-Martin, M.L., Gatenby, R.A., 2004. pH imaging. A review of pH measurement methods and applications in cancers. IEEE Eng. Med. Biol. Mag. 23, 57–64.

Hobbs, S.K., Monsky, W.L., Yuan, F., Roberts, W.G., Griffith, L., Torchilin, V.P., Jain, R.K., 1998. Regulation of transport pathways in tumor vessels: role of tumor type and microenvironment. Proc. Natl. Acad. Sci. U.S.A. 95, 4607–4612.

Huang, M., Ma, Z., Khor, E., Lim, L.Y., 2002. Uptake of FITC-chitosan nanoparticles by A549 cells. Pharm. Res. 19, 1488–1494.

Kataoka, K., Harada, A., Nagasaki, Y., 2001. Block copolymer micelles for drug delivery: design, characterization and biological significance. Adv. Drug Deliv. Rev. 47, 113–131.

Kim, G.M., Bae, Y.H., Jo, W.H., 2005. pH-induced micelle formation of poly(histidine-co-phenylalanine)-block-poly(ethylene glycol) in aqueous media. Macromol. Biosci. 5, 1118–1124.

Kim, D., Lee, E.S., Oh, K.T., Gao, Z.G., Bae, Y.H., 2008. Doxorubicin-loaded polymeric micelle overcomes multidrug resistance of cancer by double-targeting folate receptor and early endosomal pH. Small 4, 2043–2050.

Lavasanifar, A., Samuel, J., Kwon, G.S., 2002. Poly(ethylene oxide)-block-poly(L-amino acid) micelles for drug delivery. Adv. Drug Deliv. Rev. 54, 169–190.

Lee, E.S., Youn, Y.S., 2008. Poly(benyzl-L-histidine)-b-poly(ethylene glycol) micelle engineered for tumor acidic pH-targeting, in vitro evaluation. Bull. Korean Chem. Soc. 29, 1539–1544.

Lee, E.S., Na, K., Bae, Y.H., 2003. Polymeric micelle for tumor pH and folate-mediated targeting. J. Control. Release 91, 103–113.

Lee, E.S., Na, K., Bae, Y.H., 2005a. Doxorubicin loaded pH-sensitive polymeric micelles for reversal of resistant MCF-7 tumor. J. Control. Release 103, 405–418.

Lee, E.S., Na, K., Bae, Y.H., 2005b. Super pH-sensitive multifunctional polymeric micelle. Nano Lett. 5, 325–329.

Lee, E.S., Oh, K.T., Kim, D., Youn, Y.S., Bae, Y.H., 2007a. Tumor pH-responsive flower-like micelles of poly(L-lactic acid)-b-poly(ethylene glycol)-b-poly(L-histidine). J. Control. Release 123, 19–26.

Lee, Y., Fukushima, S., Bae, Y., Hiki, S., Ishii, T., Kataoka, K., 2007b. A protein nanocarrier from charge-conversion polymer in response to endosomal pH. J. Am. Chem. Soc. 129, 5362–5363.

Lee, E.S., Kim, D., Youn, Y.S., Oh, K.T., Bae, Y.H., 2008a. A virus-mimetic nanogel vehicle13. Angew. Chem. Int. Ed. 47, 2418–2421.

Lee, E.S., Gao, Z., Kim, D., Park, K., Kwon, I.C., Bae, Y.H., 2008b. Super pH-sensitive multifunctional polymeric micelle for tumor pH(e) specific TAT exposure and multidrug resistance. J. Control. Release 129, 228–236.

Leeper, D.B., Engin, K., Thistlethwaite, A.J., Hitchon, H.D., Dover, J.D., Li, D.J., Tupchong, L., 1994. Human tumor extracellular pH as a function of blood glucose concentration. Int. J. Radiat. Oncol. Biol. Phys. 28, 935–943.

Maeda, H., Wu, J., Sawa, T., Matsumura, Y., Hori, K., 2000. Tumor vascular permeability and the EPR effect in macromolecular therapeutics: a review. J. Control. Release 65, 271–284.

Na, K., Lee, E.S., Bae, Y.H., 2007. Self-organized nanogels responding to tumor extracellular pH: pH-dependent drug release and in vitro cytotoxicity against MCF-7 cells. Bioconjug. Chem. 18, 1568–1574.

Oh, K.T., Lee, E.S., 2008. Cancer-associated pH-responsive tetracopolymeric micelles composed of poly(ethylene glycol)-b-poly(L-histidine)-b-poly(L-lactic acid)-b-poly(ethylene glycol). Polym. Adv. Technol. 19, 1907–1913.

Oh, K.T., Yin, H., Lee, E.S., Bae, Y.H., 2007. Polymeric nanovehicles for anticancer drugs with triggering release mechanisms. J. Mater. Chem. 17, 3987–4001.

Ojugo, A.S., McSheehy, P.M., McIntyre, D.J., McCoy, C., Stubbs, M., Leach, M.O., Judson, I.R., Griffiths, J.R., 1999. Measurement of the extracellular pH of solid tumours in mice by magnetic resonance spectroscopy: a comparison of exogenous (19)F and (31)P probes. NMR Biomed. 12, 495–504.

Parker, N., Turk, M.J., Westrick, E., Lewis, J.D., Low, P.S., Leamon, C.P., 2005. Folate receptor expression in carcinomas and normal tissues determined by a quantitative radioligand binding assay. Anal. Biochem. 338, 284–293.

Rothenberg, M.L., Carbone, D.P., Johnson, D.H., 2003. Improving the evaluation of new cancer treatments: challenges and opportunities. Nat. Rev. Cancer 3, 303–309.

Rybak, S.M., 2008. Antibody-onconase conjugates: cytotoxicity and intracellular routing. Curr. Pharm. Biotechnol. 9, 226–230.

Sawant, R.M., Hurley, J.P., Salmaso, S., Kale, A., Tolcheva, E., Levchenko, T.S., Torchilin, V.P., 2006. SMART drug delivery systems: double-targeted pH-responsive pharmaceutical nanocarriers. Bioconjug. Chem. 17, 943–949.

Stubbs, M., McSheehy, P.M., Griffiths, J.R., Bashford, C.L., 2000. Causes and consequences of tumour acidity and implications for treatment. Mol. Med. Today 6, 15–19.

Tannock, I.F., Rotin, D., 1989. Acid pH in tumors and its potential for therapeutic exploitation. Cancer Res. 49, 4373–4384.

van Dijk-Wolthuis, W.N.E., van de Water, L., van de Wetering, P., van Steenbergen, M.J., van den Bosch, J.J.K., Schuyl, W.J.W., Hennink, W.E., 1997. Synthesis and characterization of poly-L-lysine with controlled low molecular weight. Macromol. Chem. Phys. 198, 3893–3906.

van Sluis, R., Bhujwalla, Z.M., Raghunand, N., Ballesteros, P., Alvarez, J., Cerdan, S., Galons, J.P., Gillies, R.J., 1999. In vivo imaging of extracellular pH using 1H MRSI. Magn. Reson. Med. 41, 743–750.

Volk, T., Jahde, E., Fortmeyer, H.P., Glusenkamp, K.H., Rajewsky, M.F., 1993. pH in human tumour xenografts: effect of intravenous administration of glucose. Br. J. Cancer 68, 492–500.